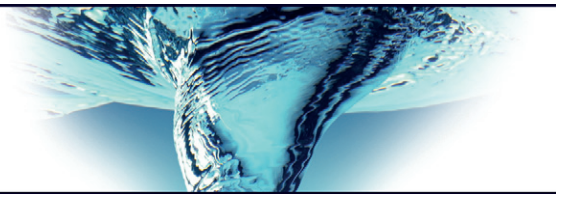
CrossMark

J. Fluid Mech. (2016), *vol.* 802, R3, doi:10.1017/jfm.2016.454



JFM RAPIDS
journals.cambridge.org/rapids

On mixing a density interface by a bubble plume

Iran E. Lima Neto[1,2], Silvana S. S. Cardoso[2] and Andrew W. Woods[1,2,†]

[1]BP Institute, University of Cambridge, Madingley Road, Cambridge CB3 0EZ, UK

[2]Department of Chemical Engineering and Biotechnology, University of Cambridge, Pembroke Street, Cambridge CB2 3RA, UK

(Received 25 March 2016; revised 24 May 2016; accepted 2 July 2016; first published online 3 August 2016)

We describe new experiments in which a bubble plume, produced from a point source of bubbles, rises through an ambient fluid composed of two layers of fluid of different density. In the lower layer, the speed of the plume exceeds the bubble rise speed and the motion is well described using classical theory of turbulent buoyant plumes. As the mixture enters the upper layer, it is either buoyant and rises to the top of the layer, or is negatively buoyant and forms a fountain. In our experiments, in which a fountain forms in the upper layer, the bubble rise speed exceeds the characteristic speed of this fountain, and a separated flow develops. The bubbles rise to the top of the system, while the lower layer fluid in the fountain rises a finite distance into the upper layer, entrains some of the upper layer fluid, and then collapses. This mixture of fluids then feeds a growing layer of density which is intermediate between the upper and lower layer. The height of rise of the fountain scales with the square of the Froude number of the fountain and the rate of entrainment of upper layer fluid into the fountain is directly proportional to the height of the fountain. This is analogous to the scaling for single-phase fountains with Froude numbers in the same range, $1 < Fr < 7$, but the constants of proportionality are smaller. We illustrate the relevance of the work for the design of mixing and aeration systems in freshwater reservoirs.

Key words: bubble dynamics, gas/liquid flow, plumes/thermals

1. Introduction

Bubble plumes have been used to destratify and mix freshwater reservoirs for many years (McDougall 1978; Wuest, Brooks & Imboden 1992; McGinnis *et al.* 2004; Kim *et al.* 2010). Numerous experiments have been conducted to explore the dynamics of such bubble plumes in both the cases with relatively small bubbles, for

†Email address for correspondence: andy@bpi.cam.ac.uk

© Cambridge University Press 2016

https://doi.org/10.1017/jfm.2016.454 Published online by Cambridge University Press

which the slip is unimportant, and larger bubbles, for which the effects of slip are more important and lead to a radially stratified flow and a reduction in the mixing efficiency of the plume (Milgram 1983; McGinnis *et al.* 2004). Models of the mixing of density-stratified reservoirs by such bubble plumes have emerged following the pioneering work of Baines & Turner (1969). They studied the filling-box flow which arises from the entrainment of ambient fluid into a single-phase turbulent buoyant plume rising through a confined environment with initially uniform density. The plume convects all the entrained fluid to the top of the reservoir, and this produces a downward flow in the environment to replenish the fluid which has been entrained. Models of such mixing by single-phase plumes have been developed to account for both two-layer (Kumagai 1984; Mott & Woods 2009) and continuously stratified ambient fluid (Cardoso & Woods 1993). In the case of a two-layer stratification, the plume may either become relatively dense at the interface, where it then forms a fountain which collapses back to the interface, generating an intermediate mixed layer, or it may continue rising into the upper layer with a reduced buoyancy. In the latter case, the mixed layer grows from the top down, whereas in the former case, the mixed layer grows at the interface. In a continuously stratified system, the plume tends to rise to a neutral buoyancy height. The filling-box flow then mixes the fluid below this height, while the stratified fluid above this mixed layer is gradually entrained as the buoyancy of the mixed layer builds up (Cardoso & Woods 1993).

By analogy, the mixing of a stratified system by a bubble plume has some similarities with a single-phase plume; a very intense bubble plume may rise to the top of the layer and mix the system from the top down, whereas a weaker bubble plume may intrude either at the interface between the layers in a two-layer system, or at a neutral buoyancy height in a continuously stratified system (Kumagai 1984; Ansong, Kyba & Sutherland 2008; Mott & Woods 2009; Camassa *et al.* 2016). Baines & Leitch (1992), Asaeda & Imberger (1993), Socolofsky & Adams (2003) and Socolofsky & Adams (2005) explored the dynamics of a bubble plume which intrudes into the ambient fluid at its neutral height in a continuously stratified system. In this case, as the neutrally buoyant fluid spreads out laterally, the bubbles tend to rise from the flow, leading to formation of a new plume of bubbles above the intrusion level. This in turn entrains ambient fluid and, depending on the depth of the ambient fluid, it may reach a second neutral level higher in the system. Chen & Cardoso (2000) explored the mixing of a two-layer stratification by a plume of very small bubbles produced by electrolysis. Their experiments led to a relatively weak fountaining flow at the interface, with the Froude number of the plume fluid just above the interface, $u/(g'r)^{1/2}$, being less than unity, where u is the plume speed, g' the reduced gravity relative to the upper layer and r the plume radius. Baines & Leitch (1992) also studied the mixing produced by a bubble plume in a two-layer stratification, but again, in their study, the flow supplied by the plume to the interface had small Froude number.

However, experiments on single-phase fountains (Turner 1966; Baines 1975; Baines, Corriveau & Reedman 1993; Bloomfield & Kerr 1998; Friedman & Katz 2000; Lin & Linden 2005; Hunt & Burridge 2015) have identified that the height of rise and the entrainment of ambient fluid into a fountain increase with the source Froude number of the fountain. Motivated by these observations, our objective is to explore the influence of the fountain Froude number on the mixing which occurs when a bubble plume reaches a density interface and transitions into a fountain in the upper layer. We first present a series of experiments that illustrate the different cases in which a bubble plume supplied to a two-layer stratified ambient (1) is buoyant just above

https://doi.org/10.1017/jfm.2016.454 Published online by Cambridge University Press

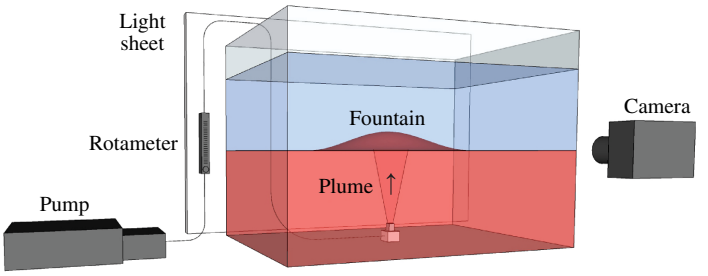


FIGURE 1. Schematic of the experimental set-up.

the interface and rises to the top of the upper layer, or (2) is negatively buoyant just above the interface and forms a fountain in the upper layer. We then test a model to predict conditions under which the bubble plume is either buoyant or relatively dense at the interface, by running a series of experiments in which we systematically reduce the density jump between the lower and upper layers. We then focus on the case in which a fountain forms in the upper layer, and quantify the resulting fountain height and the mixing of upper layer fluid into this fountain. We compare this with analogous results for a single-phase saline fountain. Finally, we explore the implications of our results for the mixing of a two-layer stratified reservoir by a bubble plume.

2. Experimental method

We carried out a series of experiments in a tank of dimension $40 \times 40 \times 50$ cm (figure 1). The tank was filled with a layer of saline water (of depth h_l and density ρ_l), then a layer of fresh water (of density ρ_u and depth h_u) was supplied above this layer. To minimise any mixing, a sponge was placed on top of the layer of saline solution, and the fresh water was supplied very slowly to the sponge, from which the fresh water slowly spread out above the salt water. As seen in the photographs of the experiment (e.g. figure 2), the initial interface was very sharp, with any intermediate mixed layer being less than 1–2 mm in thickness. The layer of fresh water was filled to a depth h_u. A source nozzle of diameter 4 mm was placed in the centre of its base, and a porous diffuser of size 1×1 cm was placed on this nozzle. Air was then supplied to the source nozzle with a flow rate Q_o in the range 5–20 cc s^{-1} using a peristaltic pump (Watson Marlow), leading to the production of a steady source of small bubbles from the top of the diffuser. As the bubbles rose from the air supply nozzle, a turbulent plume developed, entraining ambient fluid.

The tank was backlit using a light sheet (LightTape by Electro-LuminX Lighting Corp.). The lower layer of the fluid was dyed red while the upper layer remained clear. A series of mixtures of this red saline fluid and the fresh water, with intermediate salinity and dye concentration, were placed in the tank prior to the main experiment in order to generate a calibration curve to relate the degree of dilution of the saline water to the attenuation of light as recorded in a digital image of the tank using a NIKON D90 camera located on the opposite side of the tank to the light sheet. This calibration curve was then used to quantify the mixing in the tank produced by the fountain by analysing the evolution of the light intensity across the tank in a series of images taken at a frequency of 200 Hz during the main experiment (figure 1).

https://doi.org/10.1017/jfm.2016.454 Published online by Cambridge University Press

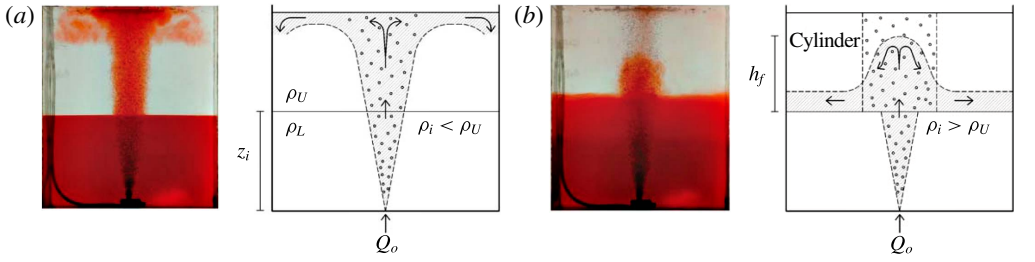


FIGURE 2. Images, from two experiments in which the plume reaches the interface, and then (*a*) continues upwards to the top of the tank, where the bubbles separate and the fluid mixes through the upper layer, or (*b*) forms a dense fountain above the interface and collapses back to the interface, forming an intermediate layer.

3. Observations of the plume in the lower layer

In the lower layer of the tank, a bubble plume was observed to develop, entraining ambient fluid and carrying it upwards (figure 2). As a result, a return flow in the ambient fluid developed, leading to a gradual descent of the top surface of the original lower layer fluid. By plotting a time series of a vertical line of pixels in the ambient fluid away from the plume, a descending front, $z = h_d(t)$, can be seen. This corresponds to the so-called first-front observed in filling-box flows (Baines & Turner 1969). By measuring the initial rate of descent of this front, $\mathrm{d}h_d/\mathrm{d}t$, in a tank with cross-sectional area A, the upward volume flux in the plume, $Q(t)$, can be estimated by the balance

$$A\frac{\mathrm{d}h_d}{\mathrm{d}t} = -Q. \tag{3.1}$$

We may quantify the buoyancy flux in the plume in terms of the source buoyancy flux gQ_b, where g is the acceleration due to gravity and Q_b is the source bubble flux. If the plume behaves as a single-phase plume with buoyancy flux B, we expect that the volume flux at height z above the source of bubbles is

$$Q(z) = \gamma B^{1/3}(z_o + z)^{5/3}, \tag{3.2}$$

where z_o is the virtual origin and γ is a constant, of value 0.15 ± 0.01, related to the entrainment coefficient α by the relation $\gamma = (6\alpha/5)(9\alpha/10)^{1/3}$ for a classical single-phase plume (Morton, Taylor & Turner 1956). By combining (3.1) and (3.2), with $z = h_d$, we can estimate γ for all of the experiments listed in table 1, and we find that $\gamma = 0.16 \pm 0.03$. This is consistent with the classical value for a turbulent buoyant plume, suggesting that the assumption that the plume behaves as a single-phase plume in the lower layer is a reasonable approximation (figure 3). In estimating γ, we estimated the virtual origin of the plume in the lower layer by estimating the location of the equivalent point source for the linearly spreading plume, given that, from plume theory, the radius of the plume follows a law of the form $r = 6\alpha/5(z_o + z)$. This suggests that $z_o \approx 2$ cm in our experiments. We note that near the actual source, the flow involves a relatively large flux of gas, but as the flow mixes with water and dilutes, the gas volume fraction decreases so that, for points 10–15 cm above the source, it has fallen to values less than 0.05, and the flow has adjusted to that of a classical Boussinesq plume. The estimate of the virtual origin implicitly accounts for this adjustment process near the source, representing the plume flow at the interface in terms of that produced from an idealised point source with the same buoyancy flux.

https://doi.org/10.1017/jfm.2016.454 Published online by Cambridge University Press

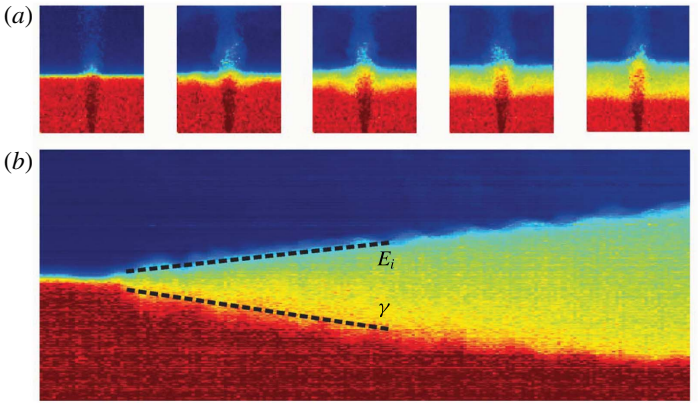


FIGURE 3. (*a*) Series of images indicating how the fountain mixes across the interface. The colour denotes the horizontally averaged salinity at each point in the tank, and indicates the gradual formation of intermediate density fluid at the interface. (*b*) Time series (horizontal) of a vertical line through the ambient fluid away from the fountain. The gradual descent of the base of the intermediate layer into the original lower layer can be used to quantify the flux of lower layer fluid which is entrained into the plume and carried into the fountain. The gradual ascent of the mixed layer can be used to quantify the rate of mixing of upper layer fluid into the collapsing fountain.

If the bubble rise speed is smaller than the plume speed in the lower layer, we expect that the flow may be approximated as a single-phase flow. To this end, we have measured the size of the bubbles produced from the nozzle used in our experiments by using high-precision analysis of the images from the experiments, and find values in the range 0.1–0.2 cm. Bubbles in this size range rising in water are ellipsoidal, and there are extensive experimental data showing that such bubbles in fact have an approximately constant rise speed of 0.23 m s^{-1} (Clift, Grace & Weber 1978). As a further check, we made independent measurements of the bubble rise speed using our high-frequency images of the experiments to track the speed of individual bubbles, and this also confirms the bubble rise speeds were in the range 0.23 ± 0.01 m s^{-1}. To estimate the horizontally averaged 'top-hat' rise speed of the fluid in the plume (cf. Morton *et al.* 1956) we use single-phase plume theory, which predicts that

$$u = kB^{1/3}(z_o + z)^{-1/3}, \tag{3.3}$$

where $k = (5/6\alpha)(9\alpha/10)^{1/3} \approx 3.84$. Substituting in the values from our experiments, we find that at the initial position of the interface between the lower and upper layers, $z = h_l$, the plume speed is larger than the rise speed of the bubbles for each experiment (diamonds, figure 4), and so we expect that the motion in the lower layer may be approximated as a single-phase plume, and that the scaling law (3.2) applies, consistent with our measurements (cf. figure 3).

4. Condition for fountain development in the upper layer

Given the model for the motion of the plume in the lower layer, we can estimate the bulk density of the plume on reaching the initial position of the interface, $z = h_l$, by using the conservation of buoyancy flux, which is equivalent to the conservation

https://doi.org/10.1017/jfm.2016.454 Published online by Cambridge University Press

Exp.	Q_o (cm^3 s^{-1})	h_l (m)	ρ_l (kg m^{-3})	Fr	Fr^*	λ	Flow regime
T1	5.0	0.2	1001.7	8.5	—	3.0	Plume
T2	5.0	0.2	1005.3	6.0	—	1.5	Plume
T3	5.0	0.2	1008.9	4.9	—	1.0	Fountain
T4	5.0	0.2	1012.5	4.2	12.2	0.8	Fountain
T5	5.0	0.1	1012.5	7.6	—	2.1	Plume
T6	10.0	0.2	1001.7	10.7	—	4.8	Plume
T7	10.0	0.2	1005.3	7.6	—	2.4	Plume
T8	10.0	0.2	1008.9	6.2	—	1.6	Plume
T9	10.0	0.2	1012.5	5.4	—	1.2	Fountain
T10	10.0	0.2	1026.8	3.8	7.0	0.6	Fountain
T11	10.0	0.3	1026.8	2.7	3.4	0.3	Fountain
T12	10.0	0.1	1026.8	6.8	—	1.6	Plume
T13	20.0	0.2	1008.9	7.8	—	2.5	Plume
T14	20.0	0.2	1012.5	6.8	—	1.9	Plume
T15	20.0	0.2	1016.1	6.1	—	1.5	Plume
T16	20.0	0.2	1019.7	5.5	—	1.2	Fountain
T17	20.0	0.2	1034.0	4.3	13.4	0.8	Fountain
T18	20.0	0.3	1008.9	5.6	—	1.3	Plume
T19	20.0	0.3	1034.0	3.1	4.1	0.4	Fountain
T20	6.5	0.2	1012.5	4.7	—	0.9	Fountain
T21	6.5	0.2	1034.0	3.0	3.9	0.4	Fountain
T22	6.5	0.3	1048.3	1.8	1.9	0.1	Fountain
T23	12.5	0.2	1034.0	3.7	6.3	0.6	Fountain
T24	12.5	0.3	1048.3	2.2	2.5	0.2	Fountain
T25	20.0	0.2	1034.0	4.3	13.4	0.8	Fountain
S1	25.0	0.1	1005.3	3.5	5.6	0.6	Fountain
S2	25.0	0.2	1005.3	2.0	2.2	0.2	Fountain
S3	25.0	0.3	1026.8	1.1	1.2	0.1	Fountain
S4	25.0	0.1	1016.1	3.0	4.0	0.4	Fountain
S5	25.0	0.1	1055.5	2.5	3.0	0.3	Fountain
S6	25.0	0.2	1034.0	1.5	1.6	0.1	Fountain

TABLE 1. Range of experimental conditions in the bubble plumes. The label T denotes two-phase bubble plume experiments, while the label S denotes single-phase experiments.

of gas flux in the lower layer. Given the relationship between the plume buoyancy g', volume flux Q and buoyancy flux B, $g'Q = B$, we expect that at $z = h_l$,

$$g'_l(h_l) = \frac{B^{2/3}}{\gamma (z_o + h_l)^{5/3}}, \tag{4.1}$$

where $g'_l(h_l) = g(\rho_l(h_l) - \rho(h_l))/\rho_{l0}$ is the buoyancy of the plume fluid relative to the lower layer, at the interface, and ρ_{l0} is a reference density, taken to be that of fresh water. On passing into the upper layer of the experimental reservoir, the buoyancy changes by the buoyancy difference between the upper and lower layer, $g'_{ul} = g'_l(h_l) - g'_u(h_l) = g(\rho_l(h_l) - \rho_u(h_l))/\rho_{l0}$ say, and so the buoyancy relative to the upper layer of the rising bubble–water mixture, which has density $\rho(h_l)$ at the interface, is given by $g'_u(h_l) = g(\rho_u(h_l) - \rho(h_l))/\rho_{l0}$. This may be expressed as

$$g'_u(h_l) = g'_l(h_l) - g'_{ul} = g'_{ul}[\lambda - 1], \tag{4.2}$$

https://doi.org/10.1017/jfm.2016.454 Published online by Cambridge University Press

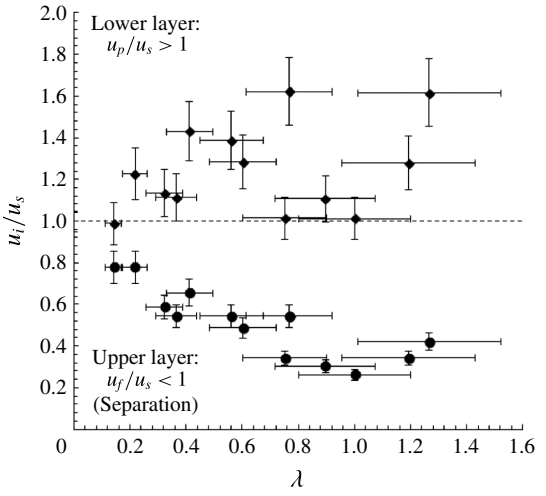


FIGURE 4. Rise speed of the fluid in the plume as a fraction of the rise speed of the bubbles (diamonds), and also the rise speed of the fluid in the fountain as a fraction of the rise speed of the bubbles (circles). Both quantities are shown as functions of the ratio of the buoyancy of the plume relative to the lower layer and the buoyancy of the upper layer relative to the lower layer, λ. If $\lambda < 1$, then on entering the upper layer the bulk density of the flow is in excess of the density of the upper layer, and the flow then evolves as a fountain in the upper layer.

where $\lambda = g'_l(h_l)/g'_{ul}(h_l)$. Equation (4.2) expresses the relation between the buoyancy of the flow above and below the interface and the buoyancy difference across the interface of the two liquid layers.

It follows that if $\lambda > 1$ then the plume fluid is still buoyant above the interface. If the continuing plume speed in the upper layer remains larger than the bubble rise speed, then we expect the plume to rise to the top of the tank (see figure 2*a*). However, we note that if the tank is very tall, then as the plume continues to rise through the upper layer, the plume speed will decrease and eventually the bubbles can separate from the fluid, leading to collapse of the remaining relatively saline fluid and formation of a fountain.

In contrast, if $\lambda < 1$, we expect the plume to transition into a collapsing fountain above the interface (cf. Kumagai 1984), with the additional complexity that the bubbles then separate from this fountain and carry on rising to the top of the tank (see figure 2*b*). In figure 5, we present the estimated value of λ for each of the experiments listed in table 1. If the flow developed into a fountain, we use solid symbols, whereas in the case that the flow reached the top of the tank, we use open symbols. The figure shows very good agreement of the predicted transition, $\lambda = 1$, with the observed transition in the behaviour of each of the flows.

Henceforth, our main focus lies in flows for which $\lambda < 1$. In this case there is a transition to fountaining behaviour in the upper layer. Our experimental observations show that the fluid bubble mixture rises above the interface and that the fluid then comes to rest some distance above the interface, while the bubbles continue to rise. To help clarify the motion of the fluid and the bubbles, in figure 6(*a*) we present a photograph of the bubble–water mixture. In this figure, it may be seen how the lower layer fluid rises a certain distance above the interface, where it then comes to rest

https://doi.org/10.1017/jfm.2016.454 Published online by Cambridge University Press

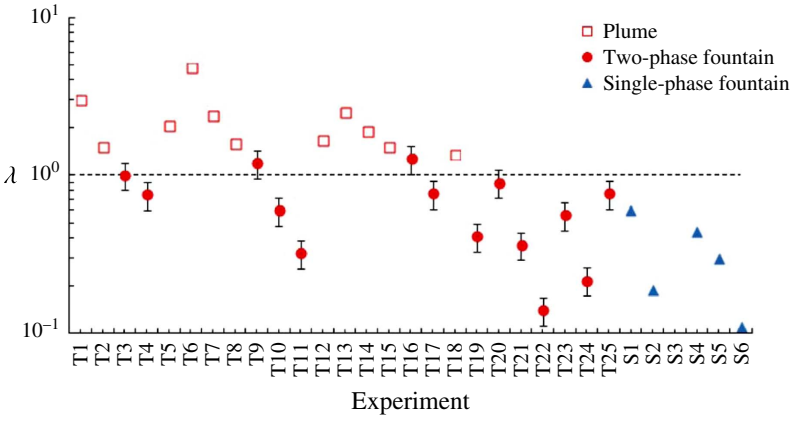


FIGURE 5. Comparison of the value of λ estimated for each of the experiments listed in table 1, with the observation of whether the experiment leads to a collapsing fountain (closed symbols) or a flow which reached the surface of the reservoir (open symbols).

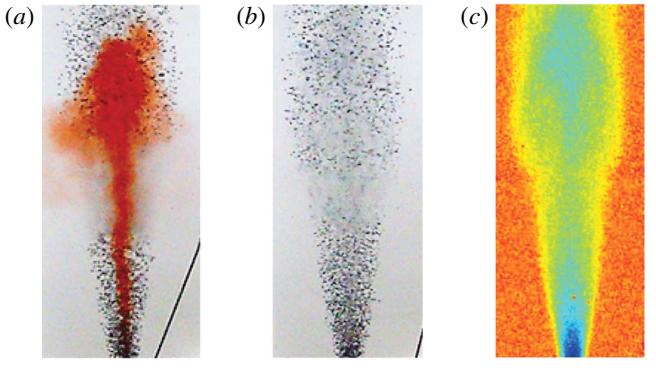


FIGURE 6. Images illustrating: (*a*) the case in which some of the fluid carried up from the lower layer is dyed red, showing how it rises a finite distance then collapses back to the interface; (*b*) bubbles rising in the plume below the interface and the fountain above the interface; and (*c*) a time-lapse image to visualise the spatial distribution of the bubbles averaged over time, in both the plume, below the interface, and the fountain, above the interface.

and falls back to the interface, mixing with some of the upper layer fluid en route. In figure 6(*b*) we present an image with no dye in the fluid, which illustrates the rise of the bubbles in both the lower layer, where they gradually spread out as predicted by the plume model, and in the upper layer, where they rise in a nearly cylindrical region above the interface with no significant change in radius with height. This zone in which the bubbles rise is illustrated more clearly in figure 6(*c*) using a false colour scheme for emphasis.

5. Height of rise and entrainment in the fountains

We have measured the height of rise of the dense fluid in the fountain and also the rate of entrainment of upper layer fluid into the fountain, by estimating the rate

https://doi.org/10.1017/jfm.2016.454 Published online by Cambridge University Press

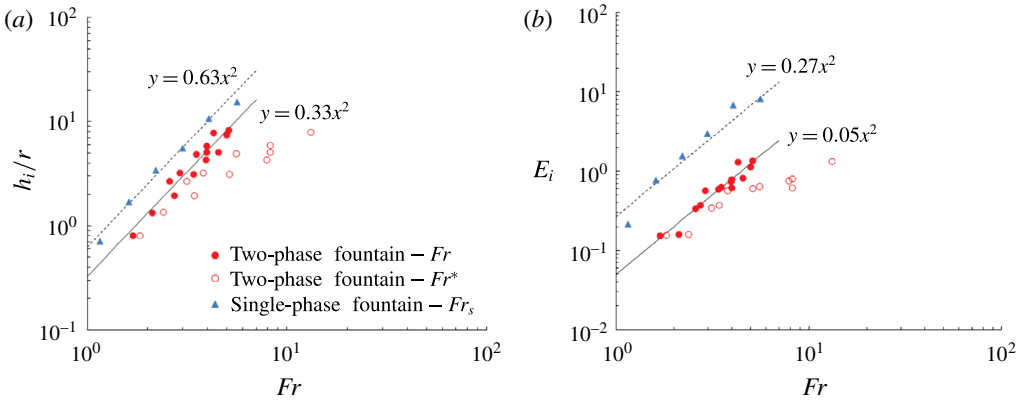


FIGURE 7. Variation of (*a*) the height of rise of the fountain and (*b*) the entrainment coefficient, as a function of the Froude number. Data are shown for the bubble fountains using the Froude number Fr, based on the density difference between the saline and fresh fluid (solid circular symbols, (5.2)), and using the Froude number Fr^*, based on the bulk density difference between the upper layer fluid and the bulk plume fluid (open circular symbols, (5.1)). Also shown in the figure are data from a series of purely single-phase experiments using fresh and saline water, shown with the blue triangular symbols, based on the Froude number Fr_s.

of ascent of the mixed layer above the interface, as shown in figure 3. In order to understand the control of each of these properties, it is useful to calculate the Froude number of the fountain, the square of which may be regarded as a measure of the ratio of the kinetic energy of the fluid in the fountain and the potential energy required to lift the fluid in the fountain a vertical distance comparable to the radius of the fountain. In defining the Froude number, there are two possible models for the buoyancy of the fountain fluid. We might consider the bulk buoyancy of the fluid, which includes the presence of the bubbles. However, on inspection of the image in figure 6 and other observations of the fountain, it is clear that the bubbles separate from the fountain liquid, and produce a region in which the bubbles rise through both the fountain liquid and the surrounding upper layer fluid. Indeed, we can estimate the characteristic speed of the fountain, based on the buoyancy and momentum flux of the fluid rising from the interface, by using the scaling for the horizontally averaged 'top-hat' fountain speed at the initial position of the interface (Turner 1966), $u_l = M^{3/4}/B^{1/2}$, where $M = u_l Q$ and $B = g'_u Q$, with Q evaluated at the interface. If we compare this speed with the rise speed of the bubbles we find that for all our experiments the rise speed of the bubbles is greater than the speed of the fountain (figure 4), and so we expect the bubbles to separate from the fountain fluid, as is indeed observed (figure 6). As a result, it may be more appropriate to define the Froude number in terms of the density difference between the lower layer and upper layer fluids. In figure 7(*a*) we illustrate the height of rise of the fountain in the upper layer, h_i, as a function of (i) a Froude number Fr^* based on the difference between the plume bulk density at the interface, $z = h_l$, and the upper layer, Fr^* shown by open circles and defined as

$$Fr^* = \frac{u_l}{(g'_u(h_l)r(h_l))^{1/2}} \tag{5.1}$$

https://doi.org/10.1017/jfm.2016.454 Published online by Cambridge University Press

and (ii) a Froude number Fr based on the density difference between the upper and lower layer fluid, shown by closed circles and defined by

$$Fr = \frac{u_l}{(g'_{ul} r(h_l))^{1/2}}, \tag{5.2}$$

where $r(h_l)$ is the radius of the plume at the interface, given by $r(h_l) = 6\alpha/5(h_l + z_o)$ and u_l is the plume speed at the interface (3.3).

In figure 7(*a*), we also present the fountain heights above the interface, h_i, obtained from a series of reference single-phase experiments we have carried out using fresh and saline fluid (shown by blue triangles). These experiments use a Froude number Fr_s based on the density difference between the plume fluid at the interface and the upper layer fluid. It is seen that the height of the single-phase fountains (triangles) and bubble fountains (solid circles) depend on Froude number according to the relations

$$h_i = (0.63 \pm 0.08) Fr_s^2 r(h_l) \quad \text{and} \quad h_i = (0.33 \pm 0.05) Fr^2 r(h_l), \tag{5.3a,b}$$

with the Froude number varying from 1–7. In contrast if we do apply the bulk buoyancy difference in our definition of the Froude number for the bubble fountains, Fr^*, we find a relation $h_i = (0.42 \pm 0.15) r(h_l) Fr^*$ (open circles) with the Froude number, Fr^*, now lying in the range 2–10. This has much more scatter than the fit (5.3*b*) using the Froude number Fr (5.2). In these expressions, $r(h_l)$ is the radius of the fountain at the initial position of the interface between the fresh and saline fluid.

An original aim of the experimental study was to determine the rate of mixing of the upper layer fluid into the fountain. We have measured this for each of the experiments by calculating the rate of ascent of the mixed layer above the interface, located at $z = h_m$ (cf. figure 3). We then define an entrainment coefficient E_i according to the relation

$$A \frac{\mathrm{d}h_m}{\mathrm{d}t} = E_i Q(h_m), \tag{5.4}$$

where $Q(h_m)$ is the plume volume flux at this upper interface. In figure 7(*b*), we illustrate the calculated value of E_i as a function of Fr and also Fr^* for each of our bubble fountain experiments, and also for the single-phase salt–freshwater experiments as a function of Fr_s. The value of $\mathrm{d}h_m/\mathrm{d}t$ is found during the initial stages of the experiment (cf. figure 3). It is seen that, for the bubble fountain and the saline fountain, E_i follows the trend

$$E_i = (0.05 \pm 0.02) Fr^2 \quad \text{and} \quad E_i \sim (0.27 \pm 0.09) Fr_s^2. \tag{5.5a,b}$$

This has the same dependence on Fr as the fountain height (5.2), and this is consistent with a picture in which the entrainment occurs around the flanks of the fountain, so that the total entrainment increases with the fountain height. Again, the collapse of the bubble plume data for E_i using Fr (solid circles) is more compelling than that using the Froude number Fr^* (open circles).

Our results for the height of rise of the single-phase fountain are consistent with data presented by Hunt & Burridge (2015), who found the relation $h_i = 0.82 Fr_s^2 r_n$ for the height of rise of a single-phase fountain issuing into a uniform layer from a source, where r_n is the size of the source nozzle. However, the constant of proportionality 0.82 is larger than in our experiments (5.3*a*). We suggest that this difference is the result of the different radial distribution of momentum and buoyancy in the fluid supplied to the fountain from the turbulent plume in the lower layer compared

https://doi.org/10.1017/jfm.2016.454 Published online by Cambridge University Press

to the flow being supplied from a nozzle as in the Burridge & Hunt experiments. Also, our single-phase fountain entrainment law is directly analogous to the results of Cardoso & Woods (1993), who found a constant of proportionality 0.25 for a single-phase plume entraining across an interface into a density-stratified fluid. It is worth noting, for reference, that data presented by Baines (1975) for the entrainment into a single-phase fountain followed a scaling Fr_s^3, but this was for smaller values of the Froude number than reported in the present work. In a study of a ventilation flow, Lin & Linden (2005) found that the entrainment coefficient E_i for a single-phase fountain had value 0.65 ± 0.1 for Froude numbers, which we estimate from their data fell within the range 1–2; this is consistent with our saline fountain data for Froude numbers in the range 1.25–1.75 (5.5*b*). For clarity, we note that when using the entrainment model for a single-phase fountain, we use the density contrast between the fountain fluid and the layer being entrained to define the Froude number.

6. Discussion

Our experiments have identified how a bubble plume rising through the lower layer of a two-layer stratified fluid may be transformed into a fountain on reaching a density interface if the fluid above the interface is less dense than the bulk density of the fountain fluid. We have also shown that if this happens then the bubbles tend to continue rising in the upper layer fluid, while the dense fluid in the fountain only rises a finite height above the interface and then collapses back to the interface, where it forms a mixed layer of intermediate density. We have demonstrated that the rate of mixing of the upper layer fluid into the fountain is proportional to the square of the Froude number of the fountain, and that this represents a fraction in the range of 0.05–0.4 of the volume flux arriving at the top of the fountain in the bubble plume for $1 < Fr < 7$. For comparison we have presented some analogous data for single-phase fountains produced by a single-phase plume penetrating the interface of a two-layer density-stratified ambient fluid, and these reference experiments are consistent with earlier work. We have shown that the two-phase fountains follow the same scaling laws with Froude number as the single-phase fountains, for both the height and entrainment rate, but that, owing to the two-phase separation effects, the coefficients relating the fountain height and the mixing to the Froude number are different for the single-phase and two-phase fountains (5.3, 5.5). In this context, it is important to emphasise that we define the Froude number of a single-phase fountain based on the density difference between the fountain fluid and the upper layer fluid into which the fountain penetrates. However, with the two-phase bubble fountain, in which the bubbles separate from the fountain, we define the Froude number based on the density contrast between the fluid in the fountain (excluding the effect of the bubbles) and the upper layer fluid; for a two-layer system, with a bubble plume, this corresponds to the density contrast between the lower and upper layer fluids. The reduction of the entrainment efficiency in a bubble fountain may arise from the slip of the bubbles relative to the liquid. This can continually change the local buoyancy of fluid parcels in the flow, and hence may tend to suppress the turbulence. In this context, we note that the entrainment in turbulent bubble plumes is known to be smaller than in the single-phase counterparts, as the slip velocity of the bubbles becomes more significant (cf. Milgram 1983).

It is interesting to apply the results to the case of mixing in a warm reservoir, such as the Acarape do Meio Reservoir in Ceara, Brazil. This is approximately 30 m deep, with a mixed layer of depth 5–10 m, which is 3–5 °C warmer than the

https://doi.org/10.1017/jfm.2016.454 Published online by Cambridge University Press

underlying water, corresponding to a density contrast of 1.0–1.2 kg m^{-3} with the typical temperature being 25 °C. We consider supplying the base of the lake with bubbles of size 0.5 cm, rise speed of order 0.3 m s^{-1}, and with a flux of order 0.004 m^3 s^{-1}. If we evaluate the properties of the equivalent single-phase plume at the interface, we predict that the speed $u_i \approx 0.44$ m s^{-1} while the radius $r \approx 2.9$ m. This suggests that the plume speed exceeds that of the bubbles, and so the flow in the lower layer may be approximated as a one-phase flow to leading order. We also predict that at the interface the bulk plume fluid is dense relative to the upper layer, with $\lambda \sim 0.8$ (cf. figure 2), so that a fountain will then develop above the interface. The characteristic speed of this fountain will be $u_f \sim 0.25$ m s^{-1}, suggesting that the bubbles can separate from the flow. We then predict that the fountain Froude number $Fr = 2.2$ and, using our experimental results, that the fountain will rise a height of approximately 3.7 m above the interface. We expect the fountain will be supplied with a volume flux of approximately 11 m^3 s^{-1} of lower layer fluid, and it will entrain a flux of approximately 2.2 m^3 s^{-1} of upper layer fluid. This will collect as a deepening mixed layer at the interface. With an array of such plumes across a lake, spaced 20–40 m apart, and hence each covering an area of 400–1600 m^2, the plumes could mix the lower and upper layers in a time of the order of 1000–4000 s.

Acknowledgements

This work was supported by the BP Institute for Multiphase Flow and the Brazilian National Council of Scientific and Technological Development (CNPq).

References

Ansong, J. K., Kyba, P. J. & Sutherland, B. R. 2008 Fountains impinging on a density interface. *J. Fluid Mech.* **595**, 115–139.

Asaeda, T. & Imberger, J. 1993 Structure of bubble plumes in linearly stratified environments. *J. Fluid Mech.* **249**, 35–57.

Baines, W., Corriveau, A. F. & Reedman, T. J. 1993 Turbulent fountains in a closed chamber. *J. Fluid Mech.* **255**, 621–646.

Baines, W. & Leitch, A. 1992 Destruction of stratification by a bubble plume. *J. Hydraul. Engng* **118** (4), 559–577.

Baines, W. & Turner, J. S. 1969 Turbulent buoyant convection from a source in a confined region. *J. Fluid Mech.* **37**, 51–80.

Baines, W. D. 1975 Entrainment by a jet or plume at a density interface. *J. Fluid Mech.* **68**, 309–320.

Bloomfield, L. J. & Kerr, R. C. 1998 Turbulent fountains in a stratified fluid. *J. Fluid Mech.* **358**, 335–356.

Camassa, R., Lin, Z., Mclaughlin, R. M., Mertins, K., Tzou, C., Walsh, J. & White, B. 2016 Optimal mixing of buoyant jets and plumes in stratified fluids: theory and experiments. *J. Fluid Mech.* **790**, 790–805.

Cardoso, S. S. S. & Woods, A. W. 1993 Mixing by a turbulent plume in a confined stratified region. *J. Fluid Mech.* **250**, 277–305.

Chen, M. H. & Cardoso, S. S. S. 2000 The mixing of liquids by low Reynolds number plumes. *Chem. Engng Sci.* **55** (14), 2585–2594.

Clift, R., Grace, J. & Weber, M. E. 1978 *Bubbles, Drops and Particles*. pp. 1–693. Academic.

Friedman, P. & Katz, J. 2000 Rise height for negatively buoyant fountains and depth of penetration for negatively buoyant jets impinging an interface. *Trans. ASME: J. Fluid. Engng* **122**, 779–782.

Hunt, G. & Burridge, H. 2015 Fountains in industry and nature. *Annu. Rev. Fluid Mech.* **47**, 195–220.

https://doi.org/10.1017/jfm.2016.454 Published online by Cambridge University Press

KIM, S., KIM, J., PARK, H. & PARK, N. 2010 Effects of bubble size and diffusing area on destratification efficiency in bubble plumes of two layer stratification. *J. Hydraul. Engng* **136** (2), 106–115.

KUMAGAI, M. 1984 Turbulent buoyant convection from a source in a confined two layered region. *J. Fluid Mech.* **147**, 105–131.

LIN, Y. & LINDEN, P. 2005 The entrainment due to a turbulent fountain at a density interface. *J. Fluid Mech.* **252**, 25–52.

MCDOUGALL, T. J. 1978 Bubble plumes in stratified environments. *J. Fluid Mech.* **85**, 655–672.

MCGINNIS, D., LORKE, A., WUEST, A., STOCKLI, A. & LITTLE, J. 2004 Interaction of a bubble plume and the near field in a stratified lake. *Water Resour. Res.* **40**, W10206.

MILGRAM, H. 1983 Mean flow in round bubble plumes. *J. Fluid Mech.* **133**, 345–376.

MORTON, B., TAYLOR, G. I. & TURNER, J. S. 1956 Turbulent gravitational convection production by instantaneous and maintained point sources of buoyancy. *Proc. R. Soc. Lond.* A **231**, 1–21.

MOTT, R. & WOODS, A. W. 2009 On the mixing in a confined stratified fluid by a turbulent buoyant plume. *J. Fluid Mech.* **623**, 149–165.

SOCOLOFSKY, S. & ADAMS, E. 2003 Liquid volume fluxes in stratified multiphase plumes. *J. Hydraul. Engng* **129** (11), 905–914.

SOCOLOFSKY, S. & ADAMS, E. 2005 Role of slip velocity in the behaviour of stratified multiphase plumes. *J. Hydraul. Engng* **131** (4), 273–282.

TURNER, J. S. 1966 Jets and plumes with negative or reversing buoyancy. *J. Fluid Mech.* **26**, 779–792.

WUEST, A., BROOKS, N. & IMBODEN, D. 1992 Bubble plume modelling for lake restoration. *Water Resour. Res.* **28**, 3235–3250.

https://doi.org/10.1017/jfm.2016.454 Published online by Cambridge University Press